

# 1 Estimation of airborne viral emission: quanta emission rate of SARS-CoV-2 for 2 infection risk assessment

3  
4 G. Buonanno<sup>1,2</sup>, L. Stabile<sup>1</sup>, L. Morawska<sup>2</sup>

5  
6 <sup>1</sup> Department of Civil and Mechanical Engineering, University of Cassino and Southern Lazio, Cassino, FR,  
7 Italy

8  
9 <sup>2</sup> International Laboratory for Air Quality and Health, Queensland University of Technology, Brisbane, Qld,  
10 Australia  
11

## 12 Abstract

13 Airborne transmission is a pathway of contagion that is still not sufficiently investigated despite the  
14 evidence in the scientific literature of the role it can play in the context of an epidemic. While the  
15 medical research area dedicates efforts to find cures and remedies to counteract the effects of a  
16 virus, the engineering area is involved in providing risk assessments in indoor environments by  
17 simulating the airborne transmission of the virus during an epidemic. To this end, virus air emission  
18 data are needed. Unfortunately, this information is usually available only after the outbreak, based  
19 on specific reverse engineering cases. In this work, a novel approach to estimate the viral load  
20 emitted by a contagious subject on the basis of the viral load in the mouth, the type of respiratory  
21 activity (e.g. breathing, speaking), respiratory physiological parameters (e.g. inhalation rate), and  
22 activity level (e.g. resting, standing, light exercise) is proposed. The estimates of the proposed  
23 approach are in good agreement with values of viral loads of well-known diseases from the  
24 literature. The quanta emission rates of an asymptomatic SARS-CoV-2 infected subject, with a viral  
25 load in the mouth of  $10^8$  copies  $\text{mL}^{-1}$ , were  $10.5$  quanta  $\text{h}^{-1}$  and  $320$  quanta  $\text{h}^{-1}$  for breathing and  
26 speaking respiratory activities, respectively, at rest. In the case of light activity, the values would  
27 increase to  $33.9$  quanta  $\text{h}^{-1}$  and  $1.03 \times 10^3$  quanta  $\text{h}^{-1}$ , respectively.

28 The findings in terms of quanta emission rates were then adopted in infection risk models to  
29 demonstrate its application by evaluating the number of people infected by an asymptomatic SARS-  
30 CoV-2 subject in Italian indoor microenvironments before and after the introduction of virus  
31 containment measures. The results obtained from the simulations clearly highlight that a key role is  
32 played by proper ventilation in containment of the virus in indoor environments.

33  
34 **Keywords:** SARS-CoV-2 (CoVID19); virus airborne transmission; indoor; ventilation; coronavirus;  
35 viral load  
36

## 37 1. Introduction

38 Expiratory human activities generate droplets, which can also carry viruses, through the atomization  
39 processes occurring in the respiratory tract when sufficiently high speeds are reached (Chao et al.,  
40 2009; Morawska, 2006). Indeed, during breathing, coughing, sneezing or laughing, toques of liquid  
41 originating from different areas of the upper respiratory tract are drawn out from the surface, pulled  
42 thin, and broken into columns of droplets of different sizes (Hickey and Mansour, 2019). The content  
43 of infectious agents expelled by an infected person depends, among other factors, on the location  
44 within the respiratory tract from which the droplets originated. In particular, air velocities high  
45 enough for atomization are produced when the exhaled air is forced out through some parts of the

46 respiratory tract which have been greatly narrowed. The front of the mouth is the site of narrowing  
47 and the most important site for atomization; since most droplets originate at the front of the mouth,  
48 the concentration of an infectious agent in the mouth (sputum) is representative of the  
49 concentration in the droplets emitted during the expiratory activities (Morawska, 2006). Thus,  
50 knowledge of the size and origin of droplets is important to understand transport of the virus via  
51 the aerosol route. Contrary to the findings of early investigations (Duguid, 1945; Jennison, 1942;  
52 Wells, 1934), subsequent studies involving optical particle detection techniques capable of  
53 measurements down to fractions of a micrometer suggested that the majority of these particles are  
54 in the sub-micrometer size range (Papineni and Rosenthal, 1997). More recently, the growing  
55 availability of higher temporal and spatial visualization methods using high-speed cameras (Tang et  
56 al., 2011), particle image velocimetry (Chao et al., 2009) and, above all, increasingly accurate particle  
57 counters (Morawska et al., 2009) allowed the detailed characterization and quantitation of droplets  
58 expelled during various forms of human respiratory exhalation flows (e.g. breathing, whispering,  
59 speaking, coughing). Therefore, in recent years a marked development has occurred both in the  
60 techniques for detecting the viral load in the mouth and in the engineering area of the numerical  
61 simulation of airborne transmission of the viral load emitted.

62 However, the problem of estimating the viral load emitted, which is fundamental for the simulation  
63 of airborne transmission, has not yet been solved. This is a missing "transfer function" that would  
64 allow the virology area, concerned with the viral load values in the mouth, to be connected with the  
65 aerosol science and engineering areas, concerned with the spread and mitigation of contagious  
66 particles.

67 A novel approach is here presented for estimating the viral load emitted by an infected individual.  
68 This approach, based on the principle of conservation of mass, represents a tool to connect the  
69 medical area, concerned with the concentration of the virus in the mouth, to the engineering area,  
70 dedicated to the simulation of the virus dispersion in the environment. On the basis of the proposed  
71 approach, the quanta emission rate data of SARS-CoV-2 were calculated as a function of different  
72 respiratory activities, respiratory parameters, and activity levels.

73 The quanta emission rate data, starting from the recently documented viral load in sputum  
74 (expressed in copies mL<sup>-1</sup>), were then applied in an acknowledged infection risk model to investigate  
75 the effectiveness of the containment measures implemented by the Italian government to reduce  
76 the spread of SARS-CoV-2. In particular, airborne transmission of SARS-CoV-2 by an asymptomatic  
77 subject within pharmacies, supermarkets, restaurants, banks, and post offices were simulated, and  
78 the reduction in the average number of infected people from one contagious person,  $R_0$ , was  
79 estimated.

## 80 **2. Materials and methods**

### 81 **2.1. Estimation of the quanta emission rate**

82 The approach proposed in the present work is based on the hypothesis that the droplets emitted  
83 by the infected subject have the same viral load as the sputum. Therefore, if the concentration of  
84 the virus in the sputum and the quantity of droplets emitted with dimensions less than 10  $\mu\text{m}$  is  
85 known, the viral load emitted can be determined through a mass balance. In particular, the viral  
86 load emitted, expressed in terms of quanta emission rate ( $ER_q$ , quanta h<sup>-1</sup>), was evaluated as:

$$87 \quad ER_q = c_v \cdot V_{br} \cdot N_{br} \cdot \int_0^{10\mu m} N_d(D) \cdot dV_d(D) \quad (1)$$

88 where  $c_v$  is the viral load in the sputum (RNA copies mL<sup>-1</sup>),  $V_{br}$  is the volume of exhaled air per breath  
89 (cm<sup>3</sup>; also known as tidal volume),  $N_{br}$  is the breathing rate (breath h<sup>-1</sup>),  $N_d$  is the droplet number  
90

91 concentration (part. cm<sup>-3</sup>), and  $V_d(D)$  is the volume of a single droplet (mL) as a function of the  
92 droplet diameter ( $D$ ). Information about the viral load in terms of quanta is essential as the quantum  
93 represents the “viral load” considered in engineering science: in other words, an infected individual  
94 constantly generates a number of infectious quanta over time, where a “quantum” is defined as the  
95 dose of airborne droplet nuclei required to cause infection in 63% of susceptible persons.  
96 The volume of the droplet ( $V_d$ ) was determined on the basis of data obtained experimentally by  
97 (Morawska et al., 2009): they measured the size distribution of droplets for different expiratory  
98 activities (e.g. breathing, whispering, counting, speaking), recognizing that such droplets present  
99 one or more modes occurring at different concentrations. In particular, in the study a particle size  
100 distribution with four channels was considered with midpoint diameters of  $D_1=0.8$ ,  $D_2=1.8$ ,  $D_3=3.5$ ,  
101 and  $D_4=5.5$   $\mu\text{m}$ . As an example, speaking was recognized as producing additional particles in modes  
102 near 3.5 and 5.5  $\mu\text{m}$ . These two modes became even more pronounced during sustained  
103 vocalization. Details of the aerosol concentrations at the four channels of the size distribution during  
104 each expiratory activity are reported in Table 1. The midpoint diameters of each channel were used  
105 to calculate the corresponding volume of the droplets.

106 **Table 1** - Droplet concentrations ( $N_i$ , part. cm<sup>-3</sup>) of the different size distribution channels during each  
107 expiratory activity measured by (Morawska et al., 2009).

Expiratory activity	$D_1$ (0.80 $\mu\text{m}$ )	$D_2$ (1.8 $\mu\text{m}$ )	$D_3$ (3.5 $\mu\text{m}$ )	$D_4$ (5.5 $\mu\text{m}$ )
Whispered counting	0.236	0.068	0.007	0.011
Voiced counting	0.110	0.014	0.004	0.002
Speaking	0.751	0.139	0.139	0.059
Breathing	0.084	0.009	0.003	0.002

108  
109 Based on the results obtained by (Morawska et al., 2009), equation (1) can be simplified as:

110 
$$ER_{q,j} = c_v \cdot IR \cdot \sum_{i=1}^4 (N_{i,j} \cdot V_i) \quad (2)$$

111 where  $j$  indicates the different expiratory activities considered (namely whispered counting, voiced  
112 counting, speaking, breathing) and  $IR$  (m<sup>3</sup> h<sup>-1</sup>) is the inhalation rate, i.e. the product of breathing  
113 rate ( $N_{br}$ ) and tidal volume ( $V_{br}$ ), which is a function of the activity level of the infected subject. The  
114 quanta emission rate from equation (2) can vary in a wide range depending on the virus  
115 concentration in the mouth, the activity level, and the different types of expiration. Regarding the  
116 inhalation rate effect, the quanta emission rate calculations are shown for three different activity  
117 levels (resting, standing, and light exercise) in which the inhalation rates, averaged between males  
118 and females, are equal to 0.36, 0.54, and 1.16 m<sup>3</sup> h<sup>-1</sup>, respectively (Adams, 1993; International  
119 Commission on Radiological Protection, 1994).

## 120 2.2. A demonstration application: the containment measures for the spread of SARS-CoV-2 in Italy

121 The pandemic of a novel human coronavirus, now named Severe Acute Respiratory Syndrome  
122 CoronaVirus 2 (SARS-CoV-2 throughout this manuscript), emerged in Wuhan (China) in late 2019  
123 and then spread rapidly in the world ([https://www.who.int/emergencies/diseases/novel-](https://www.who.int/emergencies/diseases/novel-coronavirus-2019)  
124 [coronavirus-2019](https://www.who.int/emergencies/diseases/novel-coronavirus-2019)). In Italy, an outbreak of SARS-CoV-2 infections was detected starting from 16  
125 cases confirmed in Lombardy (a northern region of Italy) on 21 February. The Italian government  
126 has issued government a decree dated 11 March 2020 concerning urgent measures to contain the  
127 contagion throughout the country. This decree regulated the lockdown of the country to counteract  
128 and contain the spread of the SARS-CoV-2 virus by suspending retail commercial activities, with the  
129 exception of the sale of food and basic necessities. It represents the starting point of a system with  
130 imposed constraints. Among the measures adopted for the containment of the virus in Italy, great  
131 importance was placed on the safe distance of 1 m (also known as “droplet distance”). This distance

132 was actually indicated by the World Health Organization as sufficient to avoid transmission by air,  
133 without any reference to the possibility of transmission over greater distances indoors  
134 (<https://www.who.int/emergencies/diseases/novel-coronavirus-2019>). With this measure, along  
135 with the opening of only primary commercial establishments (such as pharmacies, supermarkets,  
136 banks, post offices) and the closure of restaurants, the Italian government has adopted the concept  
137 of spacing (known as “social distancing”) to prevent the spread of the infection. Obviously, this limit  
138 per se would have no influence on the reduction of airborne transmission of the infection in indoor  
139 environments since this distance is compatible with the normal gathering of people in commercial  
140 establishments. Actually, on an absolutely voluntary basis, and despite the continuous denials by  
141 the government on the risk of indoor airborne transmission, commercial associations have changed  
142 the methods of accessing their commercial spaces such as restaurants, pharmacies, supermarkets,  
143 post offices, and banks; for example, by forcing customers to queue outside. It is clear that the best  
144 choice in containing an epidemic is a total quarantine which, however, appears to have enormous  
145 costs and social impacts, especially in Western countries.

146 To show the possible effect of the measures imposed by the Italian government (i.e. lockdown), the  
147 infection risk in different indoor microenvironments for the exposed population due to the presence  
148 of one contagious individual was simulated, adopting the infection risk model described in section  
149 2.2.1. In particular, the risk expressed in terms of basic reproduction number ( $R_0$ ) was derived from  
150 the quanta concentration and the infection risk; indeed,  $R_0$  represents the average number of  
151 secondary infections produced by a typical case of an infection in a population where everyone is  
152 susceptible (Rothman et al., 2008).

153 The indoor microenvironments considered here were a pharmacy, supermarket, restaurant, post  
154 office, and bank whose dimensions are summarized in Table 2. Two different exposure scenarios  
155 were simulated for each microenvironment: before lockdown (B) and after lockdown (A). In the  
156 simulation of the scenario before lockdown, the microenvironments were run with no particular  
157 recommendations; thus, people enter the microenvironments and queue indoors, often resulting in  
158 overcrowded environments. Since most of the indoor microenvironments in Italy are not equipped  
159 with mechanical ventilation systems, the simulations were performed considering two different  
160 situations: natural ventilation (a typical value for an Italian building equal to  $0.2 \text{ h}^{-1}$  was adopted,  
161 with reference to (d’Ambrosio Alfano et al., 2012; Stabile et al., 2017)) and mechanical ventilation  
162 (calculated according the national standard, UNI 10339 (UNI, 1995), as a function of the crowding  
163 index and the type of indoor microenvironment). The scenario after lockdown was tested  
164 considering the typical solutions adopted (on a voluntary basis) by the owners of stores and offices  
165 – reduced personnel, a reduced number of customers inside the microenvironment, customers  
166 forced to queue outdoors, and doors kept open. The scenario after lockdown was also tested for  
167 both natural ventilation and mechanical ventilation; in this case a slight increase in the air exchange  
168 rate (AER) for natural ventilation ( $0.5 \text{ h}^{-1}$ ) was considered in order to take into account that the door  
169 was always kept open. The restaurant was not tested in the scenario after lockdown since such  
170 commercial activity was closed down as a consequence of the lockdown. For all the scenarios  
171 considered in the simulations, the infected individual was considered to enter the  
172 microenvironment as the first customer (alone or along with other individuals according to the  
173 scenarios summarized in Table 2). All the scenarios were simulated taking into account that the virus  
174 is able to remain viable in the air for up to 3 hours post aerosolization as recently detected by (van  
175 Doremalen et al., 2020); thus, if the infected individual remained inside the environment for 10  
176 minutes (e.g. pharmacy), the calculation of the quanta concentration, infection risk, and  $R_0$  was  
177 performed for up to 3 hours and 10 minutes (named “total exposure time” in Table 2). For  
178 restaurants the calculation was performed for 3 hours considering that after 3 hours (i.e. two groups

179 remaining inside for 1 hour and 30 minutes one after the other) the microenvironment was left  
 180 empty.

181 **Table 2 - Summary of the exposure scenarios tested for the different microenvironments under**  
 182 **investigation: dimensions, ventilation conditions, number of workers and customers.**

		Pharmacy	Supermarket	Restaurant	Post office	Bank
Dimensions	Floor area (A, m <sup>2</sup> )	25	600	100	100	50
	Height (h, m)	3	3	3	3	3
	Volume (V, m <sup>3</sup> )	75	1800	300	300	150
Exposure scenario before lockdown (B)	Number of workers	5 (always present)	10 (always present)	4 (just the waiters, always present)	8 (always present)	4 (always present)
	Number and activity of the customers	<ul style="list-style-type: none"> <li>- 1 new customer per min entering the pharmacy,</li> <li>- every customer remains 10 min inside (including waiting time),</li> <li>- thus, 10 customers are simultaneously present</li> </ul>	<ul style="list-style-type: none"> <li>- 1 new customer every 30 s entering the supermarket,</li> <li>- every customer remains 30 min inside,</li> <li>- thus, 60 customers are simultaneously present</li> </ul>	<ul style="list-style-type: none"> <li>- 80 costumers every 1.5 hours,</li> <li>- restaurant working for 3 hours (evening),</li> <li>- thus, 80 customers are simultaneously present for a total number of 160 customers per evening.</li> </ul>	<ul style="list-style-type: none"> <li>- 1 new customer every 30 s entering the post office,</li> <li>- every customer remains 15 min inside (including waiting time),</li> <li>- thus, 30 customers are simultaneously present</li> </ul>	<ul style="list-style-type: none"> <li>- 1 new customer per min entering the bank,</li> <li>- every customer remains 15 min inside (including waiting time),</li> <li>- thus, 15 customers are simultaneously present</li> </ul>
	Air exchange rate (AER, h <sup>-1</sup> ) for natural ventilation (NV)	0.2	0.2	0.2	0.2	0.2
	Air exchange rate (AER, h <sup>-1</sup> ) for mechanical ventilation (MV)	2.2	1.1	9.6	2.4	2.4
	Total exposure time	3 hours and 10 minutes	3 hours and 30 minutes	3 hours	3 hours and 15 minutes	3 hours and 15 minutes
Exposure scenario after lockdown (A)	Number of workers	3 (always present)	10 (always present)	-	4 (always present)	4 (always present)
	Number and activity of the costumers	<ul style="list-style-type: none"> <li>- 2 new customers every five min entering the pharmacy,</li> <li>- every customer remains 5 min inside,</li> <li>- people forced to queue outside the pharmacy,</li> <li>- thus, 2 customers are simultaneously present</li> </ul>	<ul style="list-style-type: none"> <li>- 1 new customer per min entering the supermarket,</li> <li>- every customer remains 10 min inside,</li> <li>- people forced to queue outside the supermarket,</li> <li>- thus, 10 customers are simultaneously present</li> </ul>	-	<ul style="list-style-type: none"> <li>- 4 new customers every five min entering the post office,</li> <li>- every customer remains 10 min inside,</li> <li>- people forced to queue outside the post office,</li> <li>- thus, 4 customers are simultaneously present</li> </ul>	<ul style="list-style-type: none"> <li>- 4 new customers every five min entering the bank,</li> <li>- every customer remains 10 min inside,</li> <li>- people forced to queue outside the bank,</li> <li>- thus, 4 customers are simultaneously present</li> </ul>
	Air exchange rate (AER, h <sup>-1</sup> ) for natural ventilation (NV)	0.5	0.2	-	0.5	0.5
	Air exchange rate (AER, h <sup>-1</sup> ) for mechanical ventilation (MV)	2.2	1.1	-	2.4	2.4
	Total exposure time	3 hours and 5 minutes	3 hours and 10 minutes	3 hours	3 hours and 10 minutes	3 hours and 10 minutes

### 183 2.2.1. The infection risk model

184 The simulation of airborne transmission of SARS-CoV-2 was performed adopting the infection risk  
185 assessment typically implemented to evaluate the transmission dynamics of infectious diseases and  
186 to predict the risk of these diseases to the public. The model considered here to quantify the  
187 airborne transmitted infection risk was carried out by Gammaitoni and Nucci (Gammaitoni and  
188 Nucci, 1997) which represents an upgrade of an earlier model provided by Wells-Riley (Riley et al.,  
189 1978). This model was successfully adopted in previous papers estimating the infection risk due to  
190 other diseases (e.g. influenza, SARS, tuberculosis, rhinovirus) in different indoor microenvironments  
191 such as airplanes (Wagner et al., 2009), cars (Knibbs et al., 2011), and hospitals. The Gammaitoni  
192 and Nucci model is based on the rate of change in quanta levels through time; in particular, the  
193 differential equations for the change of quanta in a control volume as well as the initial conditions  
194 (here not reported for the sake of brevity) allowed to evaluate the quanta concentration in an  
195 indoor environment at the time  $t$ ,  $n(t)$ , as:

$$196 \quad n(t) = \frac{ER_q \cdot I}{AER \cdot V} + \left( n_0 + \frac{ER_q \cdot I}{AER} \right) \cdot \frac{e^{-AER \cdot t}}{V} \quad (\text{quanta m}^{-3}) \quad (3)$$

197 where AER ( $\text{h}^{-1}$ ) represents the air exchange rate of the space investigated,  $n_0$  represents the initial  
198 number of quanta in the space,  $I$  is the number of infectious subjects,  $V$  is the volume of the indoor  
199 environment considered, and  $ER_q$  is the abovementioned quanta emission rate ( $\text{quanta h}^{-1}$ )  
200 characteristic of the specific disease/virus under investigation.

201 The equation was derived considering the following simplifying assumptions: the quanta emission  
202 rate is considered to be constant, the latent period of the disease is longer than the time scale of  
203 the model, and the droplets are instantaneously and evenly distributed in the room (Gammaitoni  
204 and Nucci, 1997). The latter represents a key assumption for the application of the model as it  
205 considers that the air is well-mixed within the modelled space. The authors highlight that in  
206 epidemic modeling, where the target is the spread of the disease in the community, it is impossible  
207 to specify the geometries, the ventilation, and the locations of the infectious sources in each  
208 microenvironment. Therefore, adopting the well-mixed assumption is generally more reasonable  
209 than hypothesizing about specific environments and scenarios because the results must be  
210 interpreted on a statistical basis (Sze To and Chao, 2010).

211 To determine the infection risk ( $R$ , %) as a function of the exposure time ( $t$ ) of susceptible people,  
212 the quanta concentration was integrated over time through the Wells–Riley equation (Riley et al.,  
213 1978) as:

$$214 \quad R = \left( 1 - e^{-IR \int_0^T n(t) dt} \right) \quad (\%) \quad (4)$$

215 where  $IR$  is the inhalation rate of the exposed subject (which is, once again, affected by the subject's  
216 activity level) and  $T$  is the total time of exposure (h). From the infection risk  $R$ , the number of  
217 susceptible people infected after the exposure time can be easily determined by multiplying it by  
218 the number of exposed individuals. In fact, equations (3) and (4) were adopted to evaluate the  
219 infection risk of different exposure scenarios of Italian microenvironments hereinafter reported.  
220 The quanta emission rate used in the simulation of the scenario represents the average value  
221 obtained from the four expiratory activities (whispered counting, voiced counting, speaking, and  
222 breathing); the data are reported and discussed in the result sections.

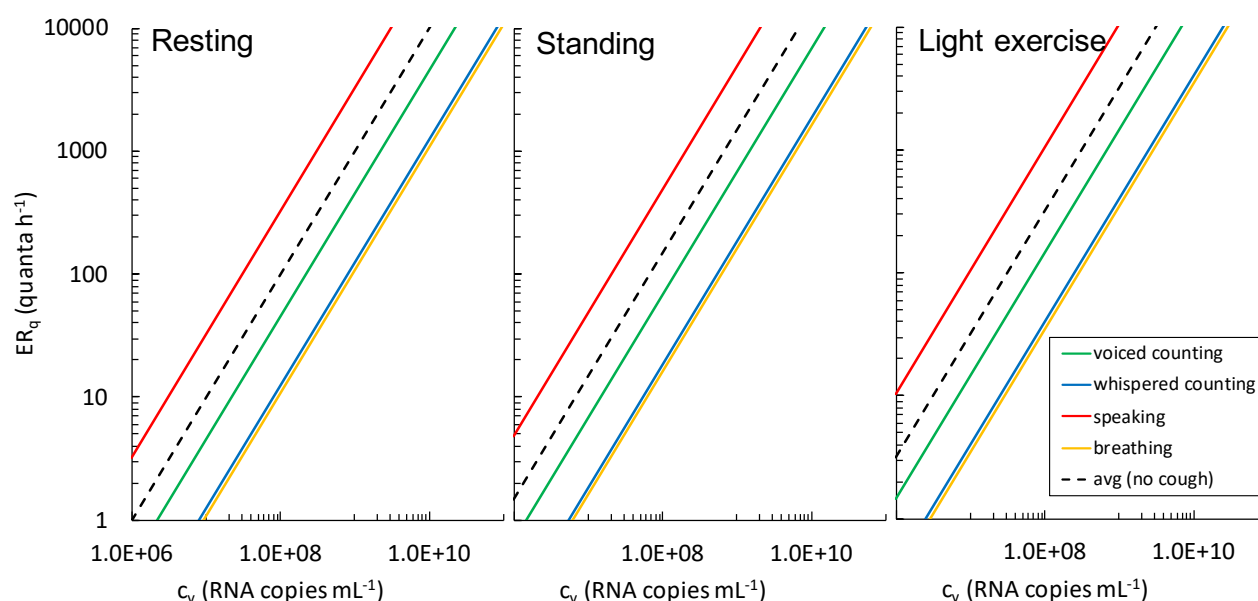
## 223 3. Results and discussions

### 224 3.1. The quanta emission rate

225 As discussed in the Materials and methods section, the quanta emission rate,  $ER_q$ , depends on  
226 several parameters. In Figure 1 the  $ER_q$  (quanta  $h^{-1}$ ) trends are reported as a function of the viral  
227 load in the sputum ( $c_v$ , RNA copies  $mL^{-1}$ ) for different expiratory activities (whispered counting,  
228 voiced counting, speaking, breathing) and different activity levels (resting, standing, light exercise).  
229 To represent the large variabilities (over several orders of magnitude) of  $ER_q$  as a function of  $c_v$ , the  
230 graph is reported on a bi-logarithmic scale.

231 To benchmark the proposed approach for the estimation of the quanta emission rate, we  
232 considered the case of seasonal influenza for which more data are available in terms of both viral  
233 load in sputum and quanta emission rate. As an example, (Hirose et al., 2016) found an average  
234 value of RNA concentration in sputum for influenza equal to  $2.38 \times 10^7$  copies  $mL^{-1}$ . Thus, applying  
235 the findings of the proposed approach in the case of a standing subject, a corresponding  $ER_q$  varying  
236 between 3.7 (breathing) and 114 quanta  $h^{-1}$  (speaking) is estimated: this value is in good agreement  
237 with the quanta emission rates for influenza found in the scientific literature, from 2 to 128  
238 quanta  $h^{-1}$  with a most frequent value of 67 quanta  $h^{-1}$  (Knibbs et al., 2012). Such variability in the  
239 quanta emission rates for influenza is due both to the method used to calculate it (Rudnick and  
240 Milton, 2003) and, especially, the viral load of the subject and the type of respiratory activity, which  
241 is typically not reported and discussed.

242



243

244 **Figure 1** -  $ER_q$  (quanta  $h^{-1}$ ) trends as a function of the viral load in sputum ( $c_v$ , RNA copies  $mL^{-1}$ ) for different  
245 respiratory activities (whispered counting, voiced counting, speaking, breathing) and different activity  
246 levels (resting, standing, light exercise). The average (avg) value of the respiratory activities considered was  
247 also reported.

248 With reference to SARS-CoV-2 infection, researchers have recently found values for the viral load in  
249 the mouth between  $10^2$  and  $10^{11}$  copies  $mL^{-1}$ , also variable in the same patient during the course of  
250 the disease (Pan et al., 2020; To et al., 2020; Woelfel et al., 2020). (Rothe et al., 2020) reported a  
251 case of SARS-CoV-2 infection acquired outside Asia in which transmission appears to have occurred  
252 during the incubation period in the index patient. A high viral load of  $10^8$  copies  $mL^{-1}$  was found,  
253 confirming that asymptomatic persons are potential sources of SARS-CoV-2 infection; this may  
254 warrant a reassessment of the transmission dynamics of the current outbreak. Table 3 lists the

255 quanta emission rates ( $ER_q$ ) for a SARS-CoV-2 infected asymptomatic subject as a function of activity  
256 level (resting, standing, and light exercise) and respiratory activity (voiced counting, whispered  
257 counting, speaking, breathing). The data confirm the huge variations in the quanta emission rate,  
258 with the lowest value being for breathing during resting activity ( $10.5 \text{ quanta h}^{-1}$ ) and the highest  
259 value being for speaking during light activity (more than  $1000 \text{ quanta h}^{-1}$ ).

260 **Table 3** – Quanta emission rates ( $ER_q$ ) for a SARS-CoV-2 infected asymptomatic subject ( $c_v=10^8 \text{ copies mL}^{-1}$ )  
261 as a function of the activity level and respiratory activity.

Activity level	Respiratory activity				
	Voiced counting	Whispered counting	Speaking	Breathing	Avg
Resting	49.9	12.1	320	10.5	98.1
Standing	74.8	18.1	480	15.7	147
Light exercise	161	39.1	$1.03 \times 10^3$	33.9	317

## 262 3.2. Results of the demonstration application

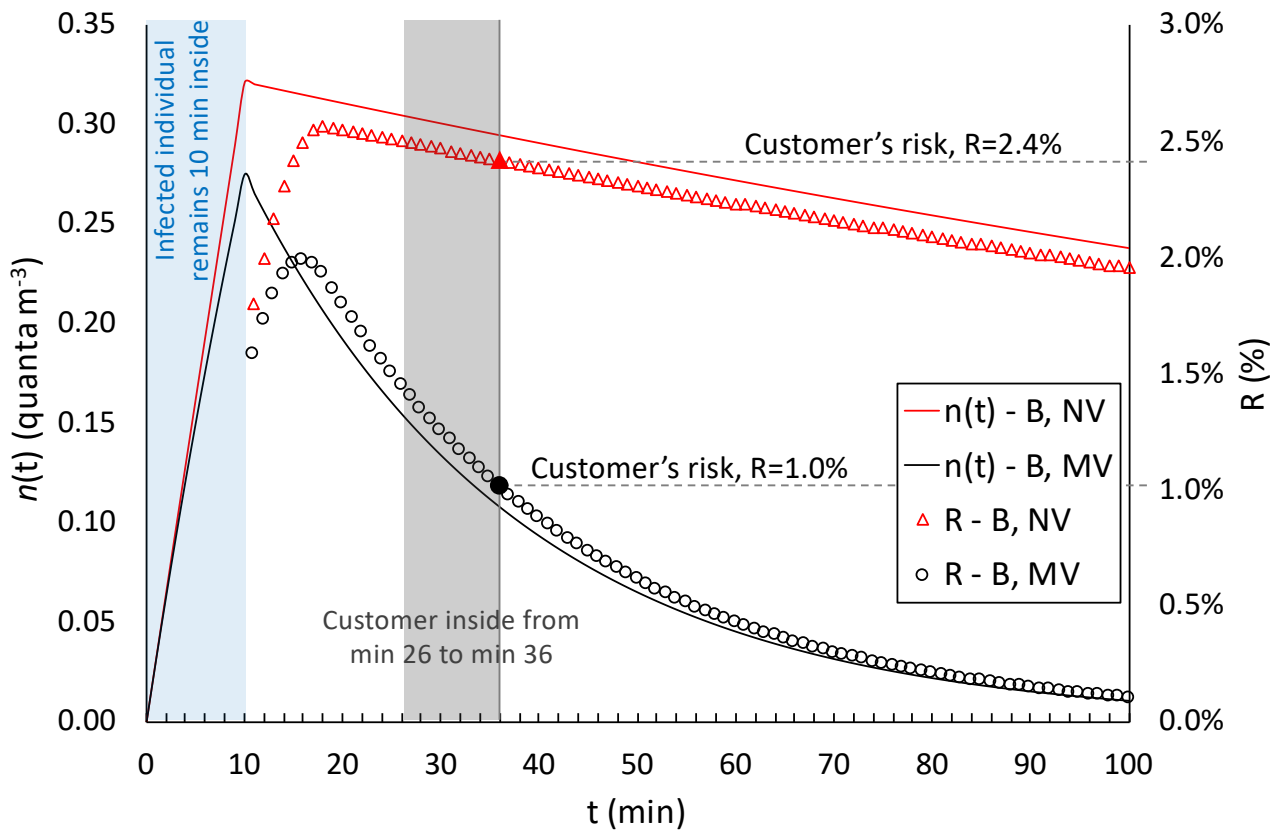
263 In this section, the results of the simulations performed for the microenvironments and exposure  
264 scenarios described in section 2.2 and summarized in Table 2 are reported.

### 265 3.2.1. Infection risk and $R_0$ for different indoor environments and exposure scenarios

266 As an illustrative example, Figure 2 shows the quanta concentration ( $n(t)$ ) and infection risk ( $R$ )  
267 trends as a function of time for two different exposure scenarios simulated for the pharmacy, i.e.  
268 before lockdown (B) in natural (NV) and mechanical ventilation (MV) conditions. The trends clearly  
269 highlight that the presence of the infected individual remaining inside for 10 minutes leads to an  
270 increase in the quanta concentration in the volume: in particular, a higher peak of quanta  
271 concentration was recognized, as expected, for reduced ventilation (NV) with respect to the  
272 mechanical ventilation (MV). People entering the pharmacy after the infected individual are  
273 exposed to a certain quanta concentration during their 10-min time, and the resulting risk for their  
274 exposure (evaluated through equation (4)) is just a function of the quanta concentration trend. For  
275 example, people entering the microenvironment around the quanta concentration peak are at a  
276 higher risk than people entering the pharmacy later. Figure 2 shows an example of a customer  
277 entering at min 26 and leaving at min 36: the risk for this 10-min exposure is 2.4% in natural  
278 ventilation conditions and 1.0% in mechanical ventilation conditions. During the entire exposure  
279 time of such a scenario (3 hours and 10 minutes), 179 customers (after the infected individual) enter  
280 the pharmacy and each of them receive their own risk. In particular, the average risk of the 179  
281 customers is 2.0% for NV conditions and 0.4% for MV conditions, then leading to a  $R_0$  (among the  
282 customers) of 3.52 and 0.68, to which must be added the  $R_0$  of the five pharmacists exposed for the  
283 entire period. Similar trends, not shown here graphically for the sake of brevity, were obtained for  
284 all the scenarios investigated, then leading to the evaluation of the  $R_0$  for each of them as described  
285 in the methodology section.

286





287  
 288 **Figure 2** - Details of application of the proposed approach in the calculation of quanta concentrations,  $n(t)$ ,  
 289 and infection risks,  $R$ , in the pharmacy environment for the exposure scenarios before lockdown (B) in  
 290 natural (NV) and mechanical ventilation (MV) conditions. The graph shows the entry of the infected  
 291 individual (first 10 minutes) and the risk for a customer entering the microenvironment at min 26 and  
 292 remaining inside for 10 minutes. The trends are shown for up to 100 minutes to highlight the peaks of the  
 293  $n(t)$  and  $R$  values.

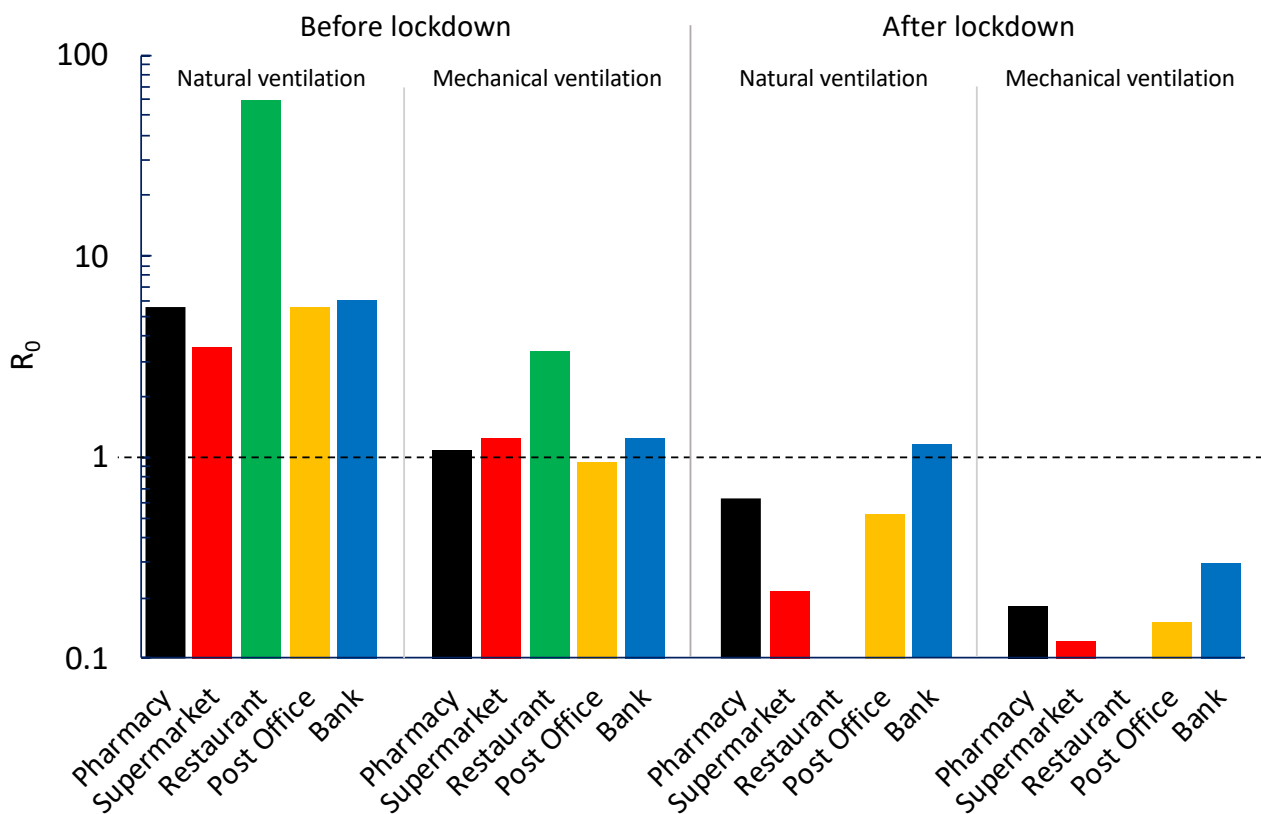
294 Figure 3 shows the reproduction number ( $R_0$ ) data calculated for all the exposure scenarios and  
 295 microenvironments under investigation (summarized in Table 2). The  $R_0$  data were calculated for an  
 296 asymptomatic SARS-CoV-2 infected subject ( $c_v=1 \times 10^8$  copies  $\text{mL}^{-1}$ ) while standing; in particular, the  
 297 average  $ER_q$  value among the different respiratory activities was considered ( $147$  quanta  $\text{h}^{-1}$ , Table  
 298 3). The exposed subjects were also considered to be standing ( $IR=0.54$   $\text{m}^3$   $\text{h}^{-1}$ ). The graph clearly  
 299 highlights some critical exposure scenarios and microenvironments. Indeed, in all the  
 300 microenvironments, a  $R_0 > 1$  was estimated for all the exposure scenarios before lockdown (B) when  
 301 the ventilation relied only upon the building being airtight (i.e. natural ventilation conditions):  $R_0$   
 302 was equal to 5.55, 3.51, 59.3, 5.59, and 6.04 for pharmacy, supermarket, restaurant, post office,  
 303 and bank, respectively. The huge value for the restaurant is obviously due to the simultaneous co-  
 304 presence of many people (80 customers and 4 waiters) and to the long exposure time (1 h and  
 305 30 min in the current simulations). This situation is obviously improved if mechanical ventilation  
 306 systems are adopted, but the  $R_0$  is still higher than 1 ( $R_0=3.40$ ). Similar results are obviously expected  
 307 for all the indoor environments characterized by high crowding indexes and long-lasting exposures  
 308 such as schools, swimming pools, gyms – venues that, in fact, were also concomitantly locked down  
 309 by the government. Actually, adopting mechanical ventilation solutions that purportedly provide an  
 310 adequate indoor air quality (i.e. providing AER values suggested by the standards (UNI, 1995)) did  
 311 not satisfactorily reduce the  $R_0$  in the other microenvironments investigated. Indeed, the  $R_0$  values  
 312 obtained from the simulations performed for the pharmacy, supermarket, post office, and bank  
 313 equipped with mechanical ventilation systems in the conditions before lockdown, with mechanical  
 314 ventilation in operation, were still  $> 1$ .

315 The new regulations and methods of accessing the indoor environments that were applied in the  
 316 conditions after lockdown (i.e. queuing outside, limited time spent in the environments, lower  
 317 crowding index) were very effective; indeed, the  $R_0$  values were reduced by roughly 80%–90% (for  
 318 both natural and mechanical ventilation conditions) with respect to the corresponding pre-  
 319 lockdown scenarios.

320 As an example, for the natural ventilation scenario, the only critical microenvironment was the bank,  
 321 since the  $R_0$  was  $>1$ ; this was due to a crowding index that was higher than the post-office, which  
 322 had a larger floor area but same number of customers. In contrast, all the  $R_0$  values for indoor  
 323 environments equipped with mechanical ventilation systems were much lower than 1 (0.18, 0.12,  
 324 0.15, and 0.30 for pharmacy, supermarket, post office, and bank, respectively). Therefore, if in a  
 325 single day the infected individual visited different environments, the resulting  $R_0$  would be lower  
 326 than 1 only if all the microenvironments were equipped with mechanical ventilation systems. Once  
 327 again, these results highlight the importance of proper ventilation of indoor environments and are  
 328 in line with the scientific literature that recognizes the importance of ventilation strategies in  
 329 reducing indoor-generated pollution (Stabile et al., 2017)(Stabile et al., 2019).

330 The values obtained with this approach could vary significantly as a function of (i) the activity levels  
 331 of both the infected subject and the exposed subjects; and (ii) the viral load in the sputum of the  
 332 infected subject; therefore, in future studies, more specific exposure scenarios could be simulated  
 333 on the basis of the findings proposed and discussed in this study.

334



335

336 **Figure 3** -  $R_0$  calculated for all the exposure scenarios (natural ventilation, mechanical ventilation; before  
 337 lockdown, after lockdown) and microenvironments (pharmacy, supermarket, restaurant, post office, bank)  
 338 under investigation considering an asymptomatic SARS-CoV-2 infected subject ( $c_v=1 \times 10^8$  copies  $mL^{-1}$ ) while  
 339 standing ( $IR=0.54 m^3 h^{-1}$ ;  $ER_q=147$  quanta  $h^{-1}$ ) and the exposed population, also standing.

340 **4. Conclusions**

341 The present study proposed the first approach aimed at filling the gap of knowledge still present in  
342 the scientific literature about evaluating the viral load emitted by infected individuals. This  
343 information could provide key information for engineers and indoor air quality experts to simulate  
344 airborne dispersion of diseases in indoor environments. To this end, we have proposed an approach  
345 to estimate the quanta emission rate (expressed in quanta h<sup>-1</sup>) on the basis of the emitted viral load  
346 from the mouth (expressed in RNA copies in mL<sup>-1</sup>), typically available from virologic analyses. Such  
347 approach also takes into account the effect of different parameters (including inhalation rate, type  
348 of respiratory activity, and activity level) on the quanta emission rate. The suitability of the findings  
349 was checked and confirmed as it was able to predict the values of quanta emission rates of previous  
350 well-known diseases in accordance with the scientific literature. The proposed approach is of great  
351 relevance as it represents an essential tool to be applied in enclosed space and it is able to support  
352 air quality experts and epidemiologists in the management of indoor environments during an  
353 epidemic just knowing its viral load, without waiting for the end of the outbreak.

354 For this purpose, it has been applied to the Italian case which, at the time of writing, represents the  
355 country with the highest number of deaths from SARS-CoV-2 in the world, highlighting the great  
356 importance of ventilation in indoor microenvironments to reduce the spread of the infection.

357

358

359 **References**

- 360 Adams, W.C., 1993. Measurement of Breathing Rate and Volume in Routinely Performed Daily Activities.  
361 Final Report. Human Performance Laboratory, Physical Education Department, University of  
362 California, Davis. Human Performance Laboratory, Physical Education Department, University of  
363 California, Davis. Prepared for the California Air Resources Board, Contract No. A033-205, April 1993.
- 364 Chao, C.Y.H., Wan, M.P., Morawska, L., Johnson, G.R., Ristovski, Z.D., Hargreaves, M., Mengersen, K., Corbett,  
365 S., Li, Y., Xie, X., Katoshevski, D., 2009. Characterization of expiration air jets and droplet size  
366 distributions immediately at the mouth opening. *Journal of Aerosol Science* 40, 122–133.  
367 <https://doi.org/10.1016/j.jaerosci.2008.10.003>
- 368 d'Ambrosio Alfano, F.R., Dell'Isola, M., Ficco, G., Tassini, F., 2012. Experimental analysis of air tightness in  
369 Mediterranean buildings using the fan pressurization method. *Building and Environment* 53, 16–25.  
370 <https://doi.org/10.1016/j.buildenv.2011.12.017>
- 371 Duguid, J.P., 1945. The numbers and the sites of origin of the droplets expelled during expiratory activities.  
372 *Edinburgh Medical Journal* LII (II), 385–401.
- 373 Gammaitoni, L., Nucci, M.C., 1997. Using a mathematical model to evaluate the efficacy of TB control  
374 measures. *Emerging Infectious Diseases* 335–342.
- 375 Hickey, A.J., Mansour, H.M., 2019. *Inhalation Aerosols: Physical and Biological Basis for Therapy*, Third  
376 Edition. Taylor & Francis Ltd.
- 377 Hirose, R., Daidoji, T., Naito, Y., Watanabe, Y., Arai, Y., Oda, T., Konishi, H., Yamawaki, M., Itoh, Y., Nakaya, T.,  
378 2016. Long-term detection of seasonal influenza RNA in faeces and intestine. *Clinical Microbiology  
379 and Infection* 22, 813.e1-813.e7. <https://doi.org/10.1016/j.cmi.2016.06.015>
- 380 International Commission on Radiological Protection, 1994. Human respiratory tract model for radiological  
381 protection. A report of a Task Group of the International Commission on Radiological Protection.  
382 *Annals of the ICRP* 24, 1–482. [https://doi.org/10.1016/0146-6453\(94\)90029-9](https://doi.org/10.1016/0146-6453(94)90029-9)
- 383 Jennison, M.W., 1942. Atomizing of mouth and nose secretions into the air as revealed by high speed  
384 photography. *Aerobiology* 17, 106–128.
- 385 Knibbs, L.D., Morawska, L., Bell, S.C., 2012. The risk of airborne influenza transmission in passenger cars.  
386 *Epidemiology and Infection* 140, 474–478. <https://doi.org/10.1017/S0950268811000835>
- 387 Knibbs, L.D., Morawska, L., Bell, S.C., Grzybowski, P., 2011. Room ventilation and the risk of airborne infection  
388 transmission in 3 health care settings within a large teaching hospital. *American Journal of Infection  
389 Control* 39, 866–872.
- 390 Morawska, L., 2006. Droplet fate in indoor environments, or can we prevent the spread of infection? *Indoor  
391 Air* 16, 335–347. <https://doi.org/10.1111/j.1600-0668.2006.00432.x>
- 392 Morawska, L., Johnson, G.R., Ristovski, Z.D., Hargreaves, M., Mengersen, K., Corbett, S., Chao, C.Y.H., Li, Y.,  
393 Katoshevski, D., 2009. Size distribution and sites of origin of droplets expelled from the human  
394 respiratory tract during expiratory activities. *Journal of Aerosol Science* 40, 256–269.  
395 <https://doi.org/10.1016/j.jaerosci.2008.11.002>
- 396 Pan, Y., Zang, D., Yang, P., Poon, L.M., Wang, Q., 2020. Viral load of SARS-CoV-2 in clinical samples Yang Pan  
397 Daitao Zhang Peng Yang Leo L M Poon Quanyi Wang. *The Lancet*.
- 398 Papineni, R.S., Rosenthal, F.S., 1997. The size distribution of droplets in the exhaled breath of healthy human  
399 subjects. *Journal of Aerosol Medicine*.
- 400 Riley, C., Murphy, G., Riley, R.L., 1978. Airborne spread of measles in a suburban elementary school. *American  
401 journal of epidemiology* 431–432.
- 402 Rothe, C., Schunk, M., Sothmann, P., Bretzel, G., Froeschl, G., Wallrauch, C., Zimmer, T., Thiel, V., Janke, C.,  
403 Guggemos, W., Seilmaier, M., Drosten, C., Vollmar, P., Zwirgmaier, K., Zange, S., Wölfel, R.,  
404 Hoelscher, M., 2020. Transmission of 2019-nCoV Infection from an Asymptomatic Contact in  
405 Germany. *N Engl J Med* 382, 970–971. <https://doi.org/10.1056/NEJMc2001468>
- 406 Rothman, K.J., Greenland, S., Lash, T.L., 2008. *Modern Epidemiology*, 3rd ed. Lippincott Williams & Wilkins.
- 407 Rudnick, S.N., Milton, D.K., 2003. Risk of indoor airborne infection transmission estimated from carbon  
408 dioxide concentration. *Indoor Air* 13, 237–245. <https://doi.org/10.1034/j.1600-0668.2003.00189.x>

409 Stabile, L., Buonanno, G., Frattolillo, A., Dell'Isola, M., 2019. The effect of the ventilation retrofit in a school  
410 on CO<sub>2</sub>, airborne particles, and energy consumptions. *Building and Environment* 156, 1–11.  
411 <https://doi.org/10.1016/j.buildenv.2019.04.001>

412 Stabile, L., Dell'Isola, M., Russi, A., Massimo, A., Buonanno, G., 2017. The effect of natural ventilation strategy  
413 on indoor air quality in schools. *Science of the Total Environment* 595, 894–902.  
414 <https://doi.org/10.1016/j.scitotenv.2017.02.030>

415 Sze To, G.N., Chao, C.Y.H., 2010. Review and comparison between the Wells–Riley and dose-response  
416 approaches to risk assessment of infectious respiratory diseases. *Indoor Air* 20, 2–16.  
417 <https://doi.org/10.1111/j.1600-0668.2009.00621.x>

418 Tang, J.W., Noakes, C.J., Nielsen, P.V., Eames, I., Nicolle, A., Li, Y., Settles, G.S., 2011. Observing and  
419 quantifying airflows in the infection control of aerosol- and airborne-transmitted diseases: an  
420 overview of approaches. *Journal of Hospital Infection* 77, 213–222.  
421 <https://doi.org/10.1016/j.jhin.2010.09.037>

422 To, K.K.-W., Tsang, O.T.-Y., Leung, W.-S., Tam, A.R., Wu, T.-C., Lung, D.C., Yip, C.C.-Y., Cai, J.-P., Chan, J.M.-C.,  
423 Chik, T.S.-H., Lau, D.P.-L., Choi, C.Y.-C., Chen, L.-L., Chan, W.-M., Chan, K.-H., Ip, J.D., Ng, A.C.-K., Poon,  
424 R.W.-S., Luo, C.-T., Cheng, V.C.-C., Chan, J.F.-W., Hung, I.F.-N., Chen, Z., Chen, H., Yuen, K.-Y., 2020.  
425 Temporal profiles of viral load in posterior oropharyngeal saliva samples and serum antibody  
426 responses during infection by SARS-CoV-2: an observational cohort study. *The Lancet Infectious  
427 Diseases*. [https://doi.org/10.1016/S1473-3099\(20\)30196-1](https://doi.org/10.1016/S1473-3099(20)30196-1)

428 UNI, 1995. UNI 10339 - Impianti aeraulici al fini di benessere. Generalità, classificazione e requisiti. Regole  
429 per la richiesta d'offerta, l'offerta, l'ordine e la fornitura.

430 van Doremalen, N., Bushmaker, T., Morris, D.H., Holbrook, M.G., Gamble, A., Williamson, B.N., Tamin, A.,  
431 Harcourt, J.L., Thornburg, N.J., Gerber, S.I., Lloyd-Smith, J.O., de Wit, E., Munster, V.J., 2020. Aerosol  
432 and Surface Stability of SARS-CoV-2 as Compared with SARS-CoV-1. *N Engl J Med*.  
433 <https://doi.org/10.1056/NEJMc2004973>

434 Wagner, B.G., Coburn, B.J., Blower, S., 2009. Calculating the potential for within-flight transmission of  
435 influenza A (H1N1). *BMC Medicine* 7, 81. <https://doi.org/10.1186/1741-7015-7-81>

436 Wells, W.F., 1934. On airborne infection: study II. Droplets and Droplet nuclei. *American Journal of  
437 Epidemiology* 20, 611–618. <https://doi.org/10.1093/oxfordjournals.aje.a118097>

438 Woelfel, R., Corman, V.M., Guggemos, W., Seilmaier, M., Zange, S., Mueller, M.A., Niemeyer, D., Vollmar, P.,  
439 Rothe, C., Hoelscher, M., Bleicker, T., Bruenink, S., Schneider, J., Ehmann, R., Zwirgmaier, K., Drosten,  
440 C., Wendtner, C., 2020. Clinical presentation and virological assessment of hospitalized cases of  
441 coronavirus disease 2019 in a travel-associated transmission cluster. *medRxiv* 2020.03.05.20030502.  
442 <https://doi.org/10.1101/2020.03.05.20030502>

443